ACS APPLIED MATERIALS & INTERFACES

Co_3O_4@MWCNT Nanocable as Cathode with Superior Electrochemical Performance for Supercapacitors

Xiaowei Wang,[†] Minxia Li,[†] Zheng Chang,[†] Yaqiong Yang,[†] Yuping Wu,*[,†,‡] and Xiang Liu*[,‡]

[†]New Energy and Materials Laboratory (NEML), Department of Chemistry & Shanghai Key Laboratory of Molecular Catalysis and Innovative Materials, Fudan University, Shanghai 200433, China

[‡]College of Energy, Nanjing Tech University, Nanjing 211816, Jiangsu Province, China

Supporting Information

ABSTRACT: Using a simple hydrothermal procedure, cobalt oxide (Co_3O_4) with preferred orientation along (220) planes is in situ prepared and coated on MWCNT. The prepared Co_3O_4@MWCNT nanocable shows superior electrochemical performance as cathode material for aqueous supercapacitors in 0.5 M KOH solution. Its redox peaks retain the well-defined shapes even when the scan rate increases to 200 mV/s. Its specific capacitance is high, 590 F/g at 15 A/g and 510 F/g even at 100 A/g within the potential range from −0.2 to 0.58 V (vs SCE). There is no capacitance fading after 2000 full cycles. This excellent performance is superior to the pristine and the reported Co_3O_4, which is ascribed to the unique nanocable structure with orientation.

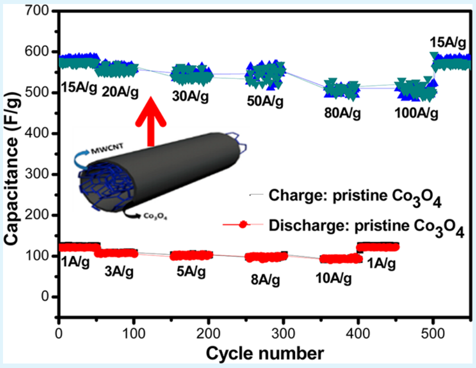

KEYWORDS: *supercapacitor, cathode, Co_3O_4@MWCNT, nanocable, rate performance*

INTRODUCTION

Recently, increasingly serious energy shortages, environmental pollution from economic development, and the increasing population have stimulated unremitting research efforts into renewable energies such as solar and wind energy.[1] However, the supply and demand for these renewable energy sources fluctuates with time and season. Therefore, the stability of power supply from these energy sources should be adjusted by energy storage systems to meet the frequent demanding changes.[1,2] Efficient energy storage systems are urgently needed to satisfy the needs of modern society and ecological concerns.[3−5] Lithium ion batteries and supercapacitors, as two major devices for electrochemical energy storage, have provided solutions in alleviating the severe situation.[6,7] In comparison with lithium ion batteries, supercapacitors or electrochemical capacitors are superior in such aspects as high power density, fast charge/discharge processes, excellent cycling behavior, and environmental friendliness.[8]

Metal oxides/hydroxides and conducting polymers are well-explored as electrode materials with high capacitance for supercapacitors, since their pseudocapacitance is much higher than that of the traditional electrical double-layer capacitance ascribed to the reversible faradic redox reactions, which are fast.[9−11] Transition metal oxides are widely studied due to variable oxidation states of metal ions which facilitate redox transitions and higher charge storage within the potential range of water decomposition. RuO_2 has been investigated as a highly suitable option featuring very good capacitive performance, but its relatively high cost and environmentally poisonous nature have triggered the exploration of lower-cost materials with comparable/superior performance and environmental affordability.[12]

Among the transition metal oxides, Co_3O_4 is found to be one of promising alternatives owing to its high theoretical specific capacitance, good redox performance, controllable size and shape, and structural identities. As the capacitance is directly linked to surface properties, its electrochemical performance is greatly influenced by any change related to the surface morphology of this electroactive material.[13,14] In addition, during the ionic insertion and extraction processes, the particle aggregation is severe, and volume expansion/contraction is large. As a result, electrode pulverization and loss of interparticle contact take place. These result in a large capacitance loss and poor cycling stability.[15,16] A variety of appealing strategies have been applied to tackle these serious fading problems, including the preparation of unique nano/microstructures such as nanotubes,[17] nanowires,[14] nanoparticles (NPs), nanorods, and octahedral cages. In the meantime, the synthesis of carbon-based Co_3O_4 nanocomposites seems to be a preferable direction.[15,18−20] To our special attention, graphene material/metal oxide composites with diverse morphologies have recently been utilized as advanced electrode materials for supercapacitors.[21,22] Also, research on carbon nanotubes/metal oxides composites for supercapacitor

Received: September 12, 2014
Accepted: January 15, 2015
Published: January 15, 2015

DOI: 10.1021/am5062272

Scheme 1. Illustration of the Preparation Process of the Co_3O_4@MWCNT Nanocable[a]

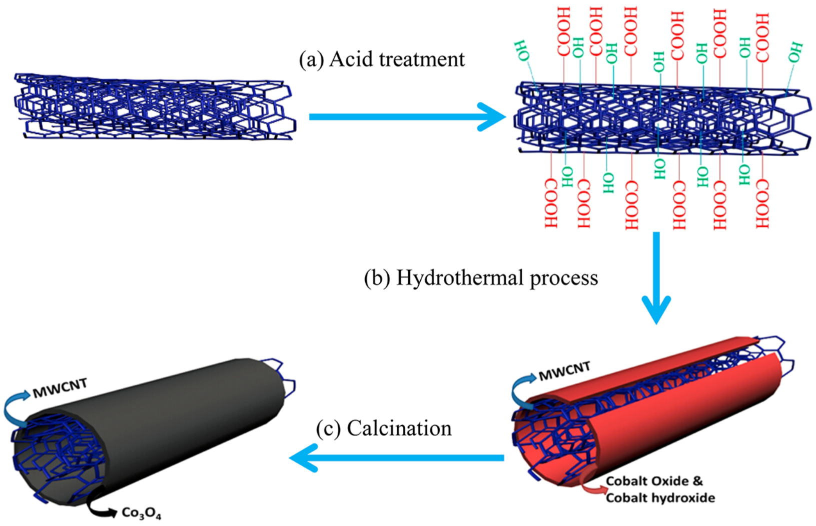

[a] (a) Acid treatment: MWCNTs were dispersed in 6 M HNO_3 for 2 h with sonication to remove the impurities and endow the surface with hydrophilic groups such as −OH and −COOH. (b) Coating Co_3O_4 on MWCNT: the acid-treated MWCNTs were immersed into an aqueous solution of $Co(Ac)_2$, and ammonia solution ($NH_3{\cdot}H_2O$, 25%) was dropwise added into the mixture solution. Then, the solution was transferred into a Teflon-lined stainless steel autoclave and heated at 150 °C for 5 h. (c) After drying at 80 °C for 12 h, a hybrid of Co_3O_4 crystal coating layer on MWCNT was obtained and then calcined at 250 °C in air atmosphere for 2 h.

applications have been reported.[23−26] These composites have demonstrated significant improvements in electrochemical properties as compared with the individual constituents.[17,18] However, the problems of rate capability and stable cycling have not been completely solved.

In this study, we designed a Co_3O_4@MWCNT nanocable by using multiwall carbon nanotubes (MWCNTs) as the core cable. Its discharge capacitance as a cathode material for supercapacitors in 0.5 M KOH aqueous solution is 590 F/g at the current density of 15 A/g. Interestingly, such a unique Co_3O_4@MWCNT nanocable presents not only superior rate performance with the capacitance of 510 F/g at 100 A/g but also good cycling without any capacitance decay, which has never been reported before to our best knowledge. Its excellent electrochemical properties are of great attraction for practical supercapacitors.

EXPERIMENTAL SECTION

The synthesis of the Co_3O_4@CNT nanocable (see experimental details in Supporting Information) is schematically presented in Scheme 1. Meanwhile, a pristine Co_3O_4 under the same hydrothermal condition was also prepared as a control.

The prepared Co_3O_4@MWCNT nanocable or pristine Co_3O_4 was mixed with acetylene black and poly(tetrafluoroethylene) (PTFE) in a weight ratio of 8:1:1 with the help of ethanol. After drying, the mixture was pressed into a film with an active mass loading of ∼6 mg/cm^2. Next, the film was cut into disks. These disks were pressed onto Ni grid at a pressure of 10 MPa and then dried at 80 °C overnight to act as working electrodes.

The cyclic voltammetry (CV) data were collected at different scan rates on an electrochemical working station CHI440B (Chenhua). A three-electrode cell consisting of the above working electrode, Ni grid as the counter electrode, and SCE as the reference electrode was used to test the charge/discharge behaviors including rate capability and cycling behavior in 0.5 M KOH aqueous solution on a cell tester (Land).

RESULTS AND DISCUSSION

Scanning electron micrograph (SEM) and transmission electron micrograph (TEM) of the Co_3O_4-coated MWCNT are shown in Figure 1a,b. Clearly, there are no other Co_3O_4 particles except the nanocables. The core MWCNT is uniformly coated with Co_3O_4, whose thickness is several nanometers (inset, Figure 1b). The pristine Co_3O_4 presents as layered sheets (Figure 1c). According to the X-ray diffraction (XRD) patterns of the MWCNT, the pristine Co_3O_4, and the Co_3O_4@MWCNT nanocable shown in Figure 1d, most peaks

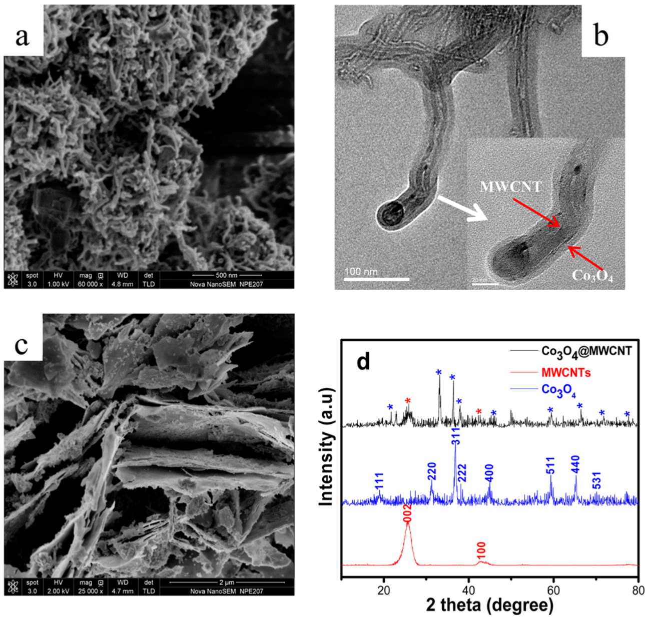

Figure 1. Characterization: (a) FESEM and (b) TEM micrographs of the prepared Co_3O_4@MWCNT nanocable; (c) SEM micrograph of the pristine layered Co_3O_4; (d) X-ray diffraction patterns of MWCNT, the pristine Co_3O_4, and the Co_3O_4@MWCNT nanocable.

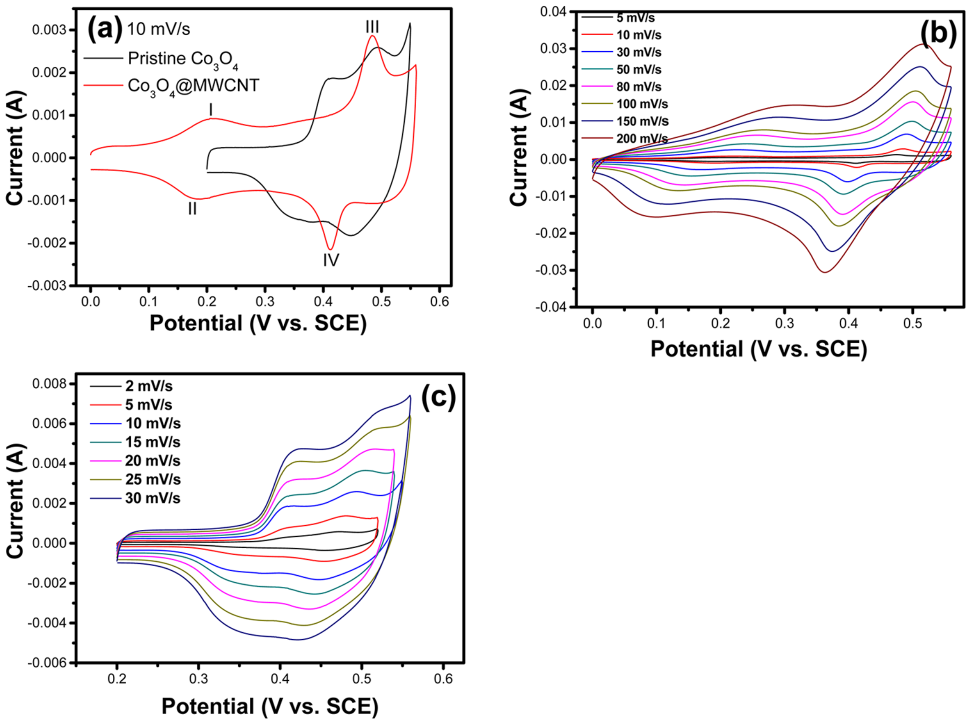

Figure 2. Cyclic voltammetric curves of the prepared materials measured using Ni as the counter electrode and SCE as the reference electrode in 0.5 M KOH aqueous solution: (a) the prepared Co_3O_4@MWCNT nanocable and the pristine Co_3O_4 at the scan rate of 10 mV/s, (b) the prepared Co_3O_4@MWCNT nanocable, and (c) the pristine Co_3O_4 at different scan rates.

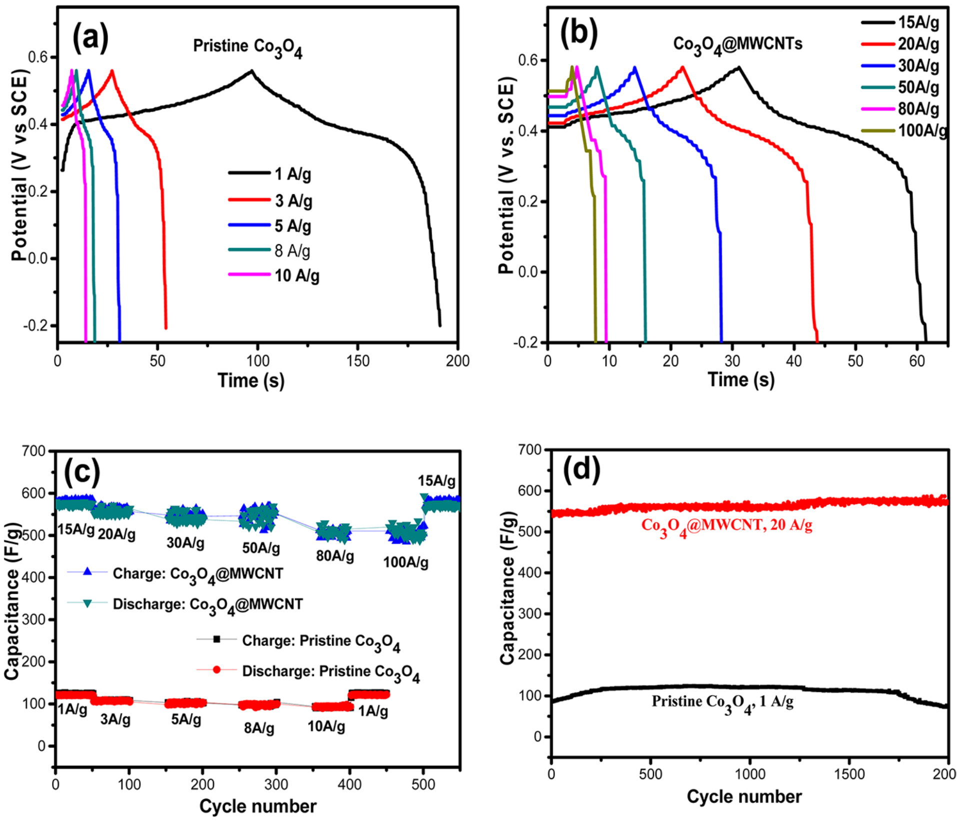

Figure 3. Electrochemical characterization of the prepared pristine Co_3O_4 and the Co_3O_4@MWCNT nanocable: Charge/discharge curves of (a) the pristine Co_3O_4 and (b) the nanocable; (c) their capacitance at different current densities; and (d) their cycling behavior.

fit very well except the (220) and (111) planes. In the pristine Co_3O_4, the intensity of (311) planes are stronger than that of the (220) ones, which is similar to the reported Co_3O_4.[19] In the prepared Co_3O_4@MWCNT nanocables, the intensity of their

(220) planes is evidently stronger than that of (311) planes. This suggests that the Co_3O_4@MWCNT structure has a crystal orientation along (220) planes. Moreover, MWCNTs consist of the graphene sheets rolled into concentric cylinders, and the π−3d orbital interaction makes it possible for the graphene plane to coordinate with Co atoms. In addition, oxygen can be compatible with the graphene plane because of the existence of −OH and −COOH groups on the surface from the acid treatment. Therefore, Co_3O_4 is orientated and deposited onto the MWCNTs by using their surface as the templates. This crystal orientation will play a vital role during the OH^- ion insertion/extraction process.

The CV curves of the pristine Co_3O_4 and the prepared Co_3O_4@MWCNT nanocable in 0.5 M KOH aqueous electrolyte are shown in Figure 2. The electrochemical windows are adjusted according to the locations of the redox couples. It can be observed that there are two redox couples at different scan rates from 5 to 200 mV/s. They are situated at 0.205/0.187 V and 0.484/0.415 V (vs saturated calomel electrode (SCE)), respectively, at 10 mV/s, resulting from the reversible transitions between Co_3O_4 and CoOOH (II/III) and between CoOOH and CoO_2 (III/IV). The reactions are presented as eqs 1 and 2.[27]

$$Co_3O_4 + OH^- + H_2O \leftrightarrow 3CoOOH + e^- \qquad (1)$$

$$CoOOH + OH^- \leftrightarrow CoO_2 + H_2O + e^- \qquad (2)$$

In the case of the pristine Co_3O_4, their potential positions are shifted a little. As to the shift or difference, it is due to their different crystal orientation since the crystal phase is the same.[19,28,29] From the comparison of the CV curves, the areas surrounded by the CV curves at the same scan rates for the nanocable are dramatically larger than those for the pristine Co_3O_4. In the meantime, the MWCNTs contribute nothing to the capacitance increase of the nanocable of Co_3O_4 with the MWCNT, which is also evidenced from the charge−discharge plot (Figure S1 in the Supporting Information). These results indicate that a large specific capacitance is associated with the nanocable and suggest that its capacitance is mainly from the pseudocapacitance of the electrochemically active Co_3O_4 instead of double-layer capacitance from the MWCNT. With the increase of the scan rate, the peak separation increases owing to the polarization. However, the peaks retain the well-defined shape even when the scan rate is as high as 200 mV/s. This is superior to the reported Co_3O_4.[18,29−33] This suggests that the nanocable will present excellent rate performance.

The rate capability and cycling behavior are shown in Figure 3. The specific capacitance is calculated as eq 3.[34]

$$C_m = I\cdot t/(\Delta V\cdot m) \qquad (3)$$

where C_m is the specific capacitance of the electrode (F/g), I is the charge/discharge current (A), t is the discharge time (s), ΔV is the potential window, and m is the mass of the electrochemically active Co_3O_4. Each datum was tested with five cells, and the average standard deviation is very small (Table S1 in the Supporting Information). In the case of the nanocable, the weight amount of Co_3O_4 is 41.88 wt % examined by thermogravimetric analysis (TG, Figure S2 in the Supporting Information). Both of them present a discharge plateau at ~0.4 V (vs SCE) corresponding to the pseudocapacitance from the redox reactions of Co_3O_4, which is similar to the above CV curves. In the case of the pristine Co_3O_4, when the current density is as high as 10 A/g, its discharge time is less than 10 s. In contrast, the nanocable can still discharge more than 30 s when the current density is as high as 15 A/g. The capacitance of the pristine Co_3O_4 is less than 130 F/g. As to the nanocable, it can be as high as 590 F/g at 15 A/g, and there is not much capacitance fading; even the current density is as high as 100 A/g (510 F/g). Also, the specific capacitance based on the total weight of the CNT/Co_3O_4 nanocable is 247 F/g at 15 A/g.[31] The superior electrochemical performance of the Co_3O_4@MWCNT nanocable is perhaps due to the larger additional amount of MWCNT compared with other work reported.[23−26] It is well-known that MWCNT is uniquely advantageous to serve as a good electronic conductor for the redox reactions to promote pseudocapacitance.[23−26] In the case of this Co_3O_4@MWCNT nanocable, this is evidenced from the Nyquist plots (see Figure S3 in the Supporting Information), which shows much lower charge-transfer resistance. In addition, the thin Co_3O_4 nanoshell markedly shortens the reaction distance, which makes the redox reactions utilized as much as possible even when the current density is very large. Also, the preferred orientation of Co_3O_4 along the (220) planes in the prepared Co_3O_4@MWCNT nanocable provides more sites vertical to (220) planes. This indicates that the insertion and extraction of OH^- becomes much easier, which is similar to the promoted intercalation/deintercalation of Li^+ ions along preferred oriented planes in $LiMn_2O_4$.[35−38] As a result, this evident excellent rate capability is superior to the reported Co_3O_4.[18,30−33,42]

In the case of the cycling behavior, the pristine Co_3O_4 shows evident capacitance decay after 1700 cycles. As to the nanocable, there is no capacitance decay after 2000 full cycles with high Coulombic efficiency (almost 100%). It is well-known that during the charge and discharge processes of Co_3O_4, there is some volume change leading to strain and stress, which result in its poor cycling behavior. In the case of our prepared Co_3O_4@MWCNT nanocable, the strain and stress can be buffered due to the thin nanostructure of Co_3O_4.[3,39−41] By the way, the flexible MWCNT can also buffer the possible change. In addition, the Co_3O_4 shell is uniformly deposited onto the MWCNT due to the actions of the hydrophilic groups such as −OH and −COOH from the pretreatment of MWCNT with nitric acid, and the combination of Co_3O_4 shell with the MWCNT core is very tight, which also leads to stable Co_3O_4 shell structure during the cycling. Consequently, the Co_3O_4@MWCNT nanocable shows superior cycling performance to the reported Co_3O_4.[18,19,30−33,42,43]

■ CONCLUSION

In summary, a Co_3O_4@MWCNT nanocable is in situ prepared by depositing Co_3O_4 on MWCNT core through a simple hydrothermal method. The thickness of the Co_3O_4 shell is only several nanometers. The nanocable retains the well-defined shapes of the redox reactions in the CV even at the scan rate of 200 mV/s. As a cathode material for supercapacitor in 0.5 M KOH aqueous solution, it presents excellent rate capability since it is capable of delivering high specific capacitance of 590 F/g at 15 A/g and still 510 F/g even at 100 A/g. Its cycling behavior is also very good, with no capacitance decay after 2000 full cycles. Its excellent electrochemical performance, which is better than the pristine and the reported Co_3O_4, is due to the electronic conductive MWCNT core, the thin Co_3O_4 nanoshell, the stable nanocable structure, and possibly preferred orientation of Co_3O_4 crystal. The Co_3O_4@MWCNT nanocable is of great promise as cathode for practical supercapacitors.

■ ASSOCIATED CONTENT

Ⓢ Supporting Information

Experimental details, charge−discharge plot of the nanocable of Co_3O_4 with MWCNT, the average standard deviation of capacitance, TG of the Co_3O_4@MWCNT nanocable, and Niquist plots of the pristine Co_3O_4 and the Co_3O_4@MWCNT nanocable. This material is available free of charge via the Internet at http://pubs.acs.org.

■ AUTHOR INFORMATION

Corresponding Authors

*Fax: +86-21-55664223. E-mail: wuyp@fudan.edu.cn. (Y.-P.W.)
*E-mail: iamxliu@njtech.edu.cn. (X.L.)

Author Contributions

The manuscript was written through contributions of all authors. All authors have given approval to the final version of the manuscript.

Notes

The authors declare no competing financial interest.

■ ACKNOWLEDGMENTS

Financial support from China National Distinguished Young Scientists (NSFC No. 51425301), STCSM (12JC1401200), and Sanyo Chem. Co. Ltd. is greatly appreciated.

■ REFERENCES

(1) Wu, Y. P.; Yuan, X. Y.; Dong, C.; Duan, J. Y. *Lithium Ion Batteries: Practice and Applications*, 2nd ed.; Chemical Industry Press: Beijing, 2012.

(2) Raja, M. W.; Mahanty, S.; Basu, R. N. Filter Paper Templated Interconnected Nanocrystalline $LiMn_2O_4$ with High Coulombic Efficiency and Rate Capability. *J. Mater. Chem.* **2009**, *19*, 6161.

(3) Arico, A. S.; Bruce, P.; Scrosati, B.; Tarascon, J. M.; Van Schalkwijk, W. Nanostructured Materials for Advanced Energy Conversion and Storage Devices. *Nat. Mater.* **2005**, *4*, 366−377.

(4) Huang, Y.; Liang, J.; Chen, Y. An Overview of the Applications of Graphene-based Materials in Supercapacitors. *Small* **2012**, *8*, 1805−34.

(5) Zhao, X.; Sanchez, B. M.; Dobson, P. J.; Grant, P. S. The Role of Nanomaterials in Redox-based Supercapacitors for Next Generation Energy Storage Devices. *Nanoscale* **2011**, *3*, 839−55.

(6) Jiang, J.; Li, Y.; Liu, J.; Huang, X.; Yuan, C.; Lou, X. W. Recent Advances in Metal Oxide-based Electrode Architecture Design for Electrochemical Energy Storage. *Adv. Mater.* **2012**, *24*, 5166−80.

(7) Simon, P.; Gogotsi, Y. Materials for Electrochemical Capacitors. *Nat. Mater.* **2008**, *7*, 845−854.

(8) Yuan, C. Z.; Gao, B.; Shen, L. F.; Yang, S. D.; Hao, L.; Lu, X. J.; Zhang, F.; Zhang, L. J.; Zhang, X. G. Hierarchically Structured Carbon-based Composites: Design, Synthesis and their Application in Electrochemical Capacitors. *Nanoscale* **2011**, *3*, 529−45.

(9) Zhang, L. L.; Zhao, X. S. Carbon-based Materials as Supercapacitor Electrodes. *Chem. Soc. Rev.* **2009**, *38*, 2520−31.

(10) Wang, G.; Zhang, L.; Zhang, J. A Review of Electrode Materials for Electrochemical Supercapacitors. *Chem. Soc. Rev.* **2012**, *41*, 797−828.

(11) Choi, N. S.; Chen, Z.; Freunberger, S. A.; Ji, X.; Sun, Y. K.; Amine, K.; Yushin, G.; Nazar, L. F.; Cho, J.; Bruce, P. G. Challenges facing Lithium Batteries and Electrical Double-layer Capacitors. *Angew. Chem., Int. Ed.* **2012**, *51*, 9994−10024.

(12) Hu, C.-C.; Chang, K.-H.; Lin, M.-C.; Wu, Y.-T. Design and Tailoring of the Nanotubular Arrayed Architecture of Hydrous RuO_2 for Next Generation Supercapacitors. *Nano Lett.* **2006**, *6*, 2690−2695.

(13) Zhu, T.; Chen, J. S.; Lou, X. W. Shape-controlled Synthesis of Porous Co_3O_4 Nanostructures for Application in Supercapacitors. *J. Mater. Chem.* **2010**, *20*, 7015−7020.

(14) Balaya, P. Size Effects and Nanostructured Materials for Energy Applications. *Energy Environ. Sci.* **2008**, *1*, 645−654.

(15) Li, Y.; Tan, B.; Wu, Y. Mesoporous Co_3O_4 Nanowire Arrays for Lithium Ion Batteries with High Capacity and Rate Capability. *Nano Lett.* **2008**, *8*, 265−270.

(16) Yao, W.-L.; Wang, J.-L.; Yang, J.; Du, G.-D. Novel Carbon Nanofiber-cobalt Oxide Composites for Lithium Storage with Large Capacity and High Reversibility. *J. Power Sources* **2008**, *176*, 369−372.

(17) Du, N.; Zhang, H.; Chen, B. D.; Wu, J. B.; Ma, X. Y.; Liu, Z. H.; Zhang, Y. Q.; Yang, D. R.; Huang, X. H.; Tu, J. P. Porous Co_3O_4 Nanotubes Derived from $Co_4(CO)_{12}$ Clusters on Carbon Nanotube Templates: A Highly Efficient Material for Li-Battery Applications. *Adv. Mater.* **2007**, *19*, 4505−4509.

(18) Wu, Z.-S.; Ren, W.; Wen, L.; Gao, L.; Zhao, J.; Chen, Z.; Zhou, G.; Li, F.; Cheng, H.-M. Graphene Anchored with Co_3O_4 Nanoparticles as Anode of Lithium Ion Batteries with Enhanced Reversible Capacity and Cyclic Performance. *ACS Nano* **2010**, *4*, 3187−3194.

(19) Dong, X.-C.; Xu, H.; Wang, X.-W.; Huang, Y.-X.; Chan-Park, M. B.; Zhang, H.; Wang, L.-H.; Huang, W.; Chen, P. 3D Graphene-Cobalt Oxide Electrode for High-Performance Supercapacitor and Enzymeless Glucose Detection. *ACS Nano* **2012**, *6*, 3206−3213.

(20) Xia, X.; Chao, D.; Fan, Z.; Guan, C.; Cao, X.; Zhang, H.; Fan, H. J. A New Type of Porous Graphite Foams and their Integrated Composites with Oxide/polymer Core/shell Nanowires for Supercapacitors: Structural design, Fabrication, and Full Supercapacitor Demonstrations. *Nano Lett.* **2014**, *14*, 1651−8.

(21) Wu, Z.-S.; Zhou, G.; Yin, L.-C.; Ren, W.; Li, F.; Cheng, H.-M. Graphene/metal Oxide Composite Electrode Materials for Energy Storage. *Nano Energy* **2012**, *1*, 107−131.

(22) Lee, J. W.; Hall, A. S.; Kim, J.-D.; Mallouk, T. E. A Facile and Template-Free Hydrothermal Synthesis of Mn_3O_4 Nanorods on Graphene Sheets for Supercapacitor Electrodes with Long Cycle Stability. *Chem. Mater.* **2012**, *24*, 1158−1164.

(23) Jiang, Y.; Wang, P.; Zang, X.; Yang, Y.; Kozinda, A.; Lin, L. Uniformly Embedded Metal Oxide Nanoparticles in Vertically Aligned Carbon Nanotube Forests as Pseudocapacitor Electrodes for Enhanced Energy Storage. *Nano Lett.* **2013**, *13*, 3524−30.

(24) Corso, B. L.; Perez, I.; Sheps, T.; Sims, P. C.; Gul, O. T.; Collins, P. G. Electrochemical Charge-transfer Resistance in Carbon Nanotube Composites. *Nano Lett.* **2014**, *14*, 1329−36.

(25) Shan, Y.; Gao, L. Multiwalled Carbon Nanotubes/Co_3O_4 Nanocomposites and Its Electrochemical Performance in Lithium Storage. *Chem. Lett.* **2004**, *33*, 1560−1561.

(26) Shan, Y.; Gao, L. Formation and Characterization of Multiwalled Carbon Nanotubes/Co_3O_4 Nanocomposites for Supercapacitors. *Mater. Chem. Phys.* **2007**, *103*, 206−210.

(27) Casella, I. G.; Gatta, M. Study of the Electrochemical Deposition and Properties of Cobalt Oxide Species in Citrate Alkaline Solutions. *J. Electroanal. Chem.* **2002**, *534*, 31−38.

(28) Mazloumi, M.; Shadmehr, S.; Rangom, Y.; Nazar, L. F.; Tang, X. Fabrication of Three-Dimensional Carbon Nanotube and Metal Oxide Hybrid Mesoporous Architectures. *ACS Nano* **2013**, *7*, 4281−4288.

(29) Wang, Y.; Lei, Y.; Li, J.; Gu, L.; Yuan, H.; Xiao, D. Synthesis of 3D-Nanonet Hollow Structured Co_3O_4 for High Capacity Supercapacitor. *ACS Appl. Mater. Interfaces* **2014**, *6*, 6739−6747.

(30) Meher, S. K.; Rao, G. R. Ultralayered Co_3O_4 for High-Performance Supercapacitor Applications. *J. Phys. Chem. C* **2011**, *115*, 15646−15654.

(31) Yuan, C.; Yang, L.; Hou, L.; Li, J.; Sun, Y.; Zhang, X.; Shen, L.; Lu, X.; Xiong, S.; Lou, X. W. D. Flexible Hybrid Paper Made of Monolayer Co_3O_4 Microsphere Arrays on rGO/CNTs and Their Application in Electrochemical Capacitors. *Adv. Funct. Mater.* **2012**, *22*, 2560−2566.

DOI: 10.1021/am5062272
ACS Appl. Mater. Interfaces 2015, 7, 2280−2285

(32) Cai, D.; Wang, D.; Liu, B.; Wang, L.; Liu, Y.; Li, H.; Wang, Y.; Li, Q.; Wang, T. Three-Dimensional Co_3O_4@$NiMoO_4$ Core/Shell Nanowire Arrays on Ni Foam for Electrochemical Energy Storage. *ACS Appl. Mater. Interfaces* **2014**, *6*, 5050−5.

(33) Wang, Y.; Zhong, Z.; Chen, Y.; Ng, C. T.; Lin, J. Controllable Synthesis of Co_3O_4 from Nanosize to Microsize with Large-scale Exposure of Active Crystal Planes and their Excellent Rate Capability in Supercapacitors Based on the Crystal Plane Effect. *Nano Res.* **2011**, *4*, 695−704.

(34) Liu, C. G.; Yu, Z. N.; Neff, D.; Zhamu, A.; Jang, B. Z. Graphene-Based Supercapacitor with an Ultrahigh Energy Density. *Nano Lett.* **2010**, *10*, 4863−4868.

(35) Tang, W.; Hou, Y. Y.; Wang, F. X.; Liu, L. L.; Wu, Y. P.; Zhu, K. $LiMn_2O_4$ Nanotube as Cathode Material of Second-Level Charge Capability for Aqueous Rechargeable Batteries. *Nano Lett.* **2013**, *13*, 2036−2040.

(36) Wang, L.; He, X. M.; Sun, W. T.; Wang, J. L.; Li, Y. D.; Fan, S. S. Crystal Orientation Tuning of $LiFePO_4$ Nanoplates for High Rate Lithium Battery Cathode Materials. *Nano Lett.* **2012**, *12*, 5632−5636.

(37) Hosono, E.; Kudo, T.; Honma, I.; Matsuda, H.; Zhou, H. S. Synthesis of Single Crystalline Spinel $LiMn_2O_4$ Nanowires for a Lithium Ion Battery with High Power Density. *Nano Lett.* **2009**, *9*, 1045−1051.

(38) Kim, J. S.; Kim, K. S.; Cho, W.; Shin, W. H.; Kanno, R.; Choi, J. W. A Truncated Manganese Spinel Cathode for Excellent Power and Lifetime in Lithium-Ion Batteries. *Nano Lett.* **2012**, *12*, 6358−6365.

(39) Maier, J. Nanoionics: Ion Transport and Electrochemical Storage in Confined Systems. *Nat. Mater.* **2005**, *4*, 805−815.

(40) Prodan, E.; Radloff, C.; Halas, N. J.; Nordlander, P. A Hybridization Model for the Plasmon Response of Complex Nanostructures. *Science* **2003**, *302*, 419−422.

(41) Li, J.; Tang, S. B.; Lu, L.; Zeng, H. C. Preparation of Nanocomposites of Metals, Metal Oxides, and Carbon Nanotubes via Self-Assembly. *J. Am. Chem. Soc.* **2007**, *129*, 9401−9409.

(42) Abdolmaleki, A.; Kazerooni, H.; Gholivand, M. B.; Heydari, H.; Pendashteh, A. Facile Electrostatic Coprecipitation of f-SWCNT/Co_3O_4 Nanocomposite as Supercapacitor Material. *Ionics* **2014**, DOI: 10.1007/s11581-014-1173-5.

(43) Gong, L. Y.; Su, L. H. Facile Synthesis of Cobalt Oxide Uniformly Coated on Multi-wall Carbon Nanotubes for Supercapacitors. *Adv. Mater. Res.* **2011**, *306−307*, 1148.